HHS Public Access

Author manuscript

Clin Cancer Res. Author manuscript; available in PMC 2016 February 02.

Published in final edited form as:

Clin Cancer Res. 2006 September 15; 12(18): 5435–5441. doi:10.1158/1078-0432.CCR-05-1773.

Tumor Hypoxia Imaging with [F-18] Fluoromisonidazole Positron Emission Tomography in Head and Neck Cancer

Joseph G. Rajendran[1,2], **David L. Schwartz**[2,3], **Janet O'Sullivan**[4], **Lanell M. Peterson**[1], **Patrick Ng**[1], **Jeffrey Scharnhorst**[1], **John R. Grierson**[1], and **Kenneth A. Krohn**[1,2]

[1]Department of Radiology, University of Washington, Washington [2]Department of Radiation Oncology, University of Washington, Washington [3]Department of Radiation Oncology, Veterans' Administration Puget Sound Health Care System, Seattle, Washington [4]University College, Cork, Cork, Ireland

Abstract

Purpose—Advanced head and neck cancer shows hypoxia that results in biological changes to make the tumor cells more aggressive and less responsive to treatment resulting in poor survival. [F-18] fluoromisonidazole (FMISO) positron emission tomography (PET) has the ability to noninvasively quantify regional hypoxia. We investigated the prognostic effect of pretherapy FMISO-PET on survival in head and neck cancer.

Experimental Design—Seventy-three patients with head and neck cancer had pretherapy FMISO-PET and 53 also had fluorodeoxyglucose (FDG) PET under a research protocol from April 1994 to April 2004.

Results—Significant hypoxia was identified in 58 patients (79%). The mean FMISO tumor/blood$_{max}$ (T/B$_{max}$) was 1.6 and the mean hypoxic volume (HV) was 40.2 mL. There were 28 deaths in the follow-up period. Mean FDG standard uptake value (SUV)$_{max}$ was 10.8. The median time for follow-up was 72 weeks. In a univariate analysis, T/B$_{max}$ ($P = 0.002$), HV ($P = 0.04$), and the presence of nodes ($P = 0.01$) were strong independent predictors. In a multivariate analysis, including FDG SUV$_{max}$, no variable was predictive at $P < 0.05$. When FDG SUV$_{max}$ was removed from the model (resulting in $n = 73$ with 28 events), nodal status and T/B$_{max}$ (or HV) were both highly predictive ($P = 0.02$, 0.006 for node and T/B$_{max}$, respectively; $P = 0.02$ and 0.001 for node and HV, respectively).

Conclusions—Pretherapy FMISO uptake shows a strong trend to be an independent prognostic measure in head and neck cancer.

Head and neck cancer is a major public health problem in the United States, affecting nearly 40,000 persons and causing ~10,000 deaths per annum, with greater incidence among the veterans. In spite of significant advances in the diagnostic methods for head and neck

Requests for reprints: Joseph Rajendran, Division of Nuclear Medicine, University of Washington, Box 356113, 1959 Pacific Street, Seattle, WA 98195. Phone: 206-598-4240; Fax: 206-598-3681; rajan@u.washington.edu.

Note: Presented at the Radiological Society of North America, Annual Meeting, Chicago, Illinois, December, 2003. Current address for D.L. Schwartz: Department of Radiation Oncology, The University of Texas M.D. Anderson Cancer Center, Houston, TX.

cancer, many patients still present in late stages with advanced disease, increasing the likelihood for developing hypoxia, a phenomenon shared with other solid tumors (1–5). Tumor hypoxia results in an aggressive phenotype, such that survival of head and neck cancer patients is significantly affected by the natural history and behavior of the hypoxic tumor cells as a result (6). A number of different treatment options are available that include surgery, radiation, and chemotherapy. Some treatment strategies are specifically directed toward overcoming the problem of hypoxia and our goal is to use imaging to identify hypoxic and therefore more aggressive cancer so that these patients could be selected for more aggressive treatment options.

Much of the published experience measuring hypoxia in patients comes from oxygen electrode studies that directly measure the tumor pO_2. Fifty percent to 60% of tumors contain hypoxic regions with $pO_2 \leq 5$ mm Hg with this technique (3, 7–9). However, the invasive nature of this approach, requiring accessible tumor sites and repeat evaluations to overcome regional heterogeneity, has limited its routine clinical use. Noninvasive positron emission tomography (PET) imaging evaluates the tumor and regional disease in a “snapshot” fashion and can provide serial quantitative measurements of hypoxia (10–13). PET imaging of tissue hypoxia using [F-18] fluoromisonidazole (FMISO), the most widely used nitro-imidazole imaging agent, was developed and validated by our group (5, 14, 15).

Positive accumulation of FMISO is proportional to the extent of hypoxia in the pO_2 range of a few mm Hg (14, 16, 17); high FMISO uptake implies a low tissue O_2 concentration.

We present here the results of our analysis of a cohort of patients with head and neck cancer who had FMISO-PET imaging before therapy. We have evaluated the ability of FMISO uptake, and by inference hypoxia, to predict survival. Some of the patients also had clinical fluorodeoxyglucose (FDG) PET and we also report complementary results for FDGPET in this subset of patients. Although FDG-PET, when available, and other clinical data were considered in planning treatment for this heterogeneous group of patients, we emphasize that all treatment was planned independent of FMISO-PET for this study. This was a purely observational study to evaluate the role of FMISO-PET hypoxia imaging for predicting survival in head and neck cancer.

Materials and Methods

Patients

A total of 73 consecutive patients with head and neck cancer were enrolled onto a FMISO-PET imaging study of patients with newly diagnosed head and neck cancer between April 1994 and April 2004. These patients underwent pretherapy FMISO and FDG-PET scans as part of several ongoing treatment protocols. Some of these patients have been included in previous abstracts (18–20). They were recruited from the Veterans’ Administration Puget Sound Health Care System, University of Washington Medical Center, and Harborview Medical Center. Signed informed consent, as approved by the University of Washington and Veterans’ Administration Puget Sound Health Care System Investigational Review Boards and radiation safety committees, was obtained in all cases.

Human use of [F-18] FMISO is covered by an Investigational New Drug authorization. Only patients with biopsy-proven cancer were included in the study. FMISO and FDG-PET studies were obtained within 2 to 3 days of each other and a few days before any therapy during the last 3 years of the study. Before this, only FMISO imaging was done. In addition to clinical examinations, all patients had routine staging procedures that included computed tomography or magnetic resonance scans, laryngoscopy, and biopsy as clinically appropriate. All evaluated patients were systematically staged following direct laryngoscopy and tissue biopsy diagnosis with plain chest radiographs, serum chemistries and liver function panels, and a contrast-enhanced computed tomography scan of the head and neck. American Joint Committee on Cancer version 6 tumor-node-metastasis criteria were used for stage delineation. Baseline staging incorporated all physical findings, diagnostic imaging (including FDG-PET findings), and available pathology results. Treatment decisions did not take into account FMISO-PET variables. All treatments were done with curative intent and consisted of definitive radiotherapy with or without chemotherapy or definitive resection with or without adjuvant radiotherapy, as recommended by a multidisciplinary tumor board.

Fifty-two patients were scheduled to receive definitive radiotherapy; 35 patients received a total radiation dose of 69.9 to 70 Gy with concurrent systemic therapy and 14 early-stage patients received a total radiation dose of 60 to 70 Gy daily single fraction radiotherapy alone. Three patients did not complete treatment. Of the 35 patients receiving chemoradiotherapy, 21 were treated according to an institutional protocol using induction and concurrent docetaxel/ carboplatin chemotherapy; 6 had chemotherapy followed by sequential radiotherapy (69.9 Gy) and 15 patients received 66 to 70 Gy daily single fraction radiotherapy with concurrent weekly taxane/carboplatin chemotherapy. Twenty-one patients underwent definitive resection and corresponding neck dissection surgery; 10 received adjuvant daily single fraction radiotherapy alone, 7 patients received both chemotherapy and radiation therapy, and 4 did not receive any adjuvant treatment following surgery. After completion of treatment, patients underwent routine surveillance every 1 to 3 months.

PET imaging

Patients were imaged in the supine position with head immobilization achieved by using moldable foam. All PET scans were done on an Advance tomograph (G.E. Medical Systems, Waukesha, WI) operating in two-dimensional, high-sensitivity mode with 35 imaging planes covering a 15 cm axial field of view. Performance characteristics of the tomograph have been published elsewhere (21, 22). Transmission scans with a Ge-68 rotating sector source were also obtained. All head and neck and torso images were reconstructed with a Hanning filter after scatter correction, resulting in a reconstructed spatial resolution of ~12 mm (21). The tomograph is regularly calibrated to convert cpm/ pixel to μCi/mL using large vials containing known activities of F-18 imaged separately from the patient and reconstructed using the same filter as the emission images.

FDG protocol

[F-18] FDG was prepared as described in the literature (23) and was injected i.v. (3.7 MBq/kg or 0.1 mCi/kg) with patients in a fasting state. All patients had blood sugar levels determined at the time of imaging (blood glucose levels should be <150 mg/dL). Patients

were not injected with FDG if the blood sugar was >150 mg/dL. Patients returned 45 minutes postinjection and were positioned in the tomograph and a scan of the tumor was obtained. Four to five axial fields of view (15 cm each) were obtained that included the base of skull and extended to at least below the liver. Emission scans, each of 7 minutes duration, followed by transmission scans of 3 minutes each were obtained. All patients were premedicated with lorazepam to reduce FDG uptake in skeletal muscle/brown fat.

FMISO protocol

[F-18] FMISO was prepared as previously described (24). Patients were not required to fast. Venous access lines were established in each arm, one for FMISO injection and the other for blood sampling. Patients were injected i.v. with 3.7 MBq/kg (0.1 mCi/kg) of [F-18] FMISO (maximum 370 MBq; 10 mCi). A single field-of-view emission scan (20 minutes) and a transmission scan (25 minutes) of the tumor region were obtained. Data acquired from ~90 to 120 minutes postinjection imaging were reconstructed to determine the tumor hypoxic volume (HV) as described below. These images were reconstructed with the same software correction and filter size used for FDG. During emission tomography, four venous blood samples were obtained at intervals of 5 minutes. Whole blood samples of 1 mL each were counted in a Cobra multichannel gamma well counter (Packard Corp., Meriden, CT) that is calibrated each week in units of cpm/μCi. Blood activity was averaged and then expressed as μCi/mL decay corrected to time of injection.

Image analysis

FDG—Images were directly processed to provide a maximum standard uptake value [SUV_{max} = maximum tissue activity (μCi/mL)/injected dose (mCi/kg)] for the tumor region. Conventional anatomic images (computed tomography, magnetic resonance) were used with side-by-side visualization to delineate tumor regions of interest for calculating the SUV. Only the primary sites of disease were included in this analysis. All imaging planes containing tumor were analyzed.

FMISO—Conventional anatomic images (computed tomography, magnetic resonance) were used with side-by side visualization to delineate tumor regions of interest, which were drawn using Alice (imaging software from HIPG, Boulder, CO) over the entire tumor volume from images transferred to a Macintosh workstation. All imaging planes containing tumor were analyzed. Data were decay corrected to the time of injection and converted to μCi/mL of tissue (T) for each pixel in the selected regions of interest. Because the blood values (B) were also expressed as μCi/mL, this allowed a pixel-by-pixel calculation of T/B activity ratio for all image planes. The number of pixels in the tumor volume with a T/B ratio ≥1.2, indicating significant hypoxia, was determined and converted to milliliter units to measure the HV. Because FMISO has a partition coefficient of almost unity in normal oxygenated tissues, the concentrations in tissue and blood rapidly equilibrate and are essentially identical. The cutoff ratio of 1.2 was based on T/B ratios previously measured with the G.E. Advance tomograph in normal human brain and muscle, where >90% of the values fell below 1.1 (12). This very simple model analysis is one of the strengths of the FMISO study. We used HV rather than fractional HV to obviate the need for delineation of tumor margins. FMISO uptake within the tumor was ensured with the help of computed tomography scans

and/or FDG-PET scans. In each tumor region, we also located the pixel with the maximum T/B ratio and include this variable, T/B_{max}, in our analysis. HV evaluates the volume of tumor that has crossed the threshold for hypoxia and T/B_{max} depicts the magnitude of hypoxia.

Statistical analysis

Death is the end point in the outcomes analysis. Of the 73 patients with survival information available, 28 deaths were recorded during the follow-up period. Survival was measured in weeks from the initial PET study. All analyses were done with standard censoring procedures for survival analysis (25). The set of prognostic variables considered in the analysis included standard clinical measures (age, tumor-node-metastasis status), as well as the PET measurements [FDG uptake, HV, and FMISO tissue to blood ratio (T/B_{max})]. The presence of distant metastasis was a strong predictor of survival, but the very limited number of patients with metastases ($n = 3$) reduces the reliability of this finding and it was therefore left out of our analyses. A square root transformation was used for the HV data to reduce the influence (leverage) of extreme points. Four values that exceeded 5 SDs were deleted (26).

Univariate analyses—Univariate analyses were done using univariate Cox regression to assess the significance of individual variables using log-rank tests. In addition, log-rank tests were used to compare Kaplan-Meier survival curves associated with patients above and below the median values for the variables of interest. Survival curves are presented with time measured in weeks.

Multivariate analyses—The relation between the time to death and the full set of measured prognostic factors was evaluated using the standard multivariate Cox proportional hazards regression analysis. This analysis permits an examination of the influence of the PET measures while controlling for the effect of other variables. The set of variables in the multivariate analysis included all those considered in the univariate setting. Age, FDG SUV_{max}, HV, and FMISO T/B_{max} were entered as continuous variables; tumor stage and nodal stage were entered as nominal variables. Due to the high correlation between HV and T/B_{max}, and the resulting issue of multicollinearity (26), these variables were each considered separately with the other prognostic variables. Two analyses were carried out. First, we considered models with FDG SUV_{max} included as a covariate. This analysis allowed us to address whether FMISO gave additional prognostic information over that of FDG SUV_{max}. A second analysis left FDG SUV_{max} out of the model. This enabled us to include an additional 21 patients where only FMISO information was available. The secondary analysis offered improved estimates of the remaining variables, and also gave some validation on the findings of the analysis that included FDG SUV_{max}. Treatment and primary tumor location varied in this data set due to patients originating from multiple protocols; however, when these variables were included in the Cox multivariate regression analyses, they were not found to alter the interpretation of other prognostic factors included in the analysis.

Results

The 73 previously untreated patients with head and neck cancer with follow-up data were analyzed for this study; all had biopsy-proven squamous cell carcinoma at the time of imaging. All patients had pretherapy FMISO-PET that was not considered in planning treatment and these were used for the primary analysis. Fifty-two patients also had pretherapy FDG-PET that was used as appropriate in planning treatment. As shown in Table 1, 27 patients had T_1 or T_2 primary tumors and 20 of these (74%) had lymph node metastases. Forty-three patients had T_3 or T_4 primary disease and 34 of them (79%) had lymph node metastases. Three patients had unevaluable (T_x) primary tumors. The primary tumor locations were as follows: 40 orophyarynx, 20 larynx, 7 oral cavity, 3 parotid, 1 maxillary sinus, and 2 unknown primary. Figure 1 is an example of FMISO and FDG images for a patient with advanced disease.

Significant hypoxia was identified in 58 patients (79%). The mean FMISO T/B_{max} was 1.6 (range 1.0–3.5) and the mean HV was 40.2 mL (range 0–1092). There were 28 deaths in the follow-up period. Mean FDG SUV_{max} was 10.8 (range 2.9–25.4). The median time from the FMISO scan to last follow-up or death was 72 weeks (range 0–521). The median follow-up of 72 weeks, although shorter than the 23 years recommended, is long enough to identify early outcome in these patients. The median follow-up for the patients who also received FDG scans was 60 weeks (range 2–143).

In the univariate analysis, T/B_{max}, HV, and nodal stage were all found to have a statistically significant ($P = 0.002$, 0.04, and 0.01, respectively) association with patient survival. However, FDG uptake, tumor stage, and age were not significant. The univariate Cox regression results are summarized in Table 2. Kaplan-Meier survival curves associated with patients above and below the median are shown in Figs. 2 to 4 (for node, T/B_{max}, and FDG SUV_{max}, respectively). Of the variables listed in Table 2, nodal status, T/B_{max}, and HV showed significant separation of the survival curves (Fig. 2 shows nodal status 2 and Fig. 3 shows T/B_{max}). Figure 4 shows the survival curve for FDG SUV_{max}, albeit with shorter follow-up than for the FMISO study.

In the multivariate analysis, we evaluated FMISO uptake (T/B_{max} and HV) combined with established prognostic indicators (nodal stage, FDG SUV_{max}, age, and tumor stage). These analyses were done with and without FDG SUV_{max}. Results for HV and T/B_{max} were similar in the multivariate setting, with T/B_{max} slightly superior. Therefore, for simplicity of presentation, we restricted our summary to only models that included T/B_{max}. Results from the model that included all prognostic factors are presented in Table 3. Here, nodal stage and T/B_{max} showed the strongest relationship with survival ($P = 0.06$); FDG SUV_{max}, which was a factor in treatment planning, also showed some association ($P = 0.08$) but the other variables were clearly not predictive. Reducing the model to those variables that were close to being significant (node, FDG SUV_{max}, and T/B_{max}), we found that P values for node remained the same, but those for FDG SUV_{max} and T/B_{max} were improved ($P = 0.05$ and $P = 0.02$, respectively).

Removing FDG SUV_{max} from the Cox regression increased the number of patients to 73 and the number of events to 28. When models that included all prognostic indicators, with the exception of FDG SUV_{max}, were considered, the conclusions regarding significant prognostic variables were not altered. The final reduced model excluded FDG SUV_{max} and is presented in Table 4; both node and T/B_{max} are highly significant.

Discussion

Tumor hypoxia has been widely implicated in poor survival of patients with cancer. Hypoxia cannot be reliably predicted by tumor size, grade, extent of necrosis, or blood hemoglobin status (5, 27). Although the negative influence of hypoxia has been recognized for decades (28), lack of a practical technique for its noninvasive evaluation has prevented hypoxia from being used as a prognostic indicator or to help direct treatment. Development of new PET tracers and increasing availability of PET imaging technology are providing tools to remedy this situation. FMISO-PET for hypoxia imaging is a robust method to estimate the burden of hypoxia in tumors.

We investigated the value of pretherapy FMISO-PET as an independent prognostic measure for predicting survival in head and neck cancer in a cohort of 73 patients with 28 deaths in the follow-up period. Two FMISO measures were used in quantifying hypoxia. The worst hypoxia was evaluated as T/B_{max}; the extent of hypoxia was quantified as the volume of pixels with a $T/B \geq 1.2$. Significant hypoxia was identified in 58 of 73 patients, and we report here the ability of FMISO uptake to predict patient survival by looking at its independent effect as well as its combined effect with established prognostic indicators. In the univariate analysis, the FMISO variables and presence of nodes were strong predictors of survival. In the multivariate analyses, FMISO imaging was more predictive than FDG. When FDG SUV_{max} was removed from the model, nodal status and T/B_{max} (or HV) were both highly predictive. The results presented here show that FMISO-PET imaging is effective in quantifying regional hypoxia in head and neck cancer. Pretherapy FMISO imaging shows a strong trend to be an independent prognostic measure in head and neck cancer, as seen in the univariate analysis and in the survival graphs.

This was a purely observational study looking at the role of FMISO-PET in head and neck cancer. As such, the influence of different tumor types and treatments on overall survival was not assessed for these independent variables. For the same reasons, we did not investigate the influence of hypoxia on locoregional disease control. Given the size of our data set and the evolving maturity of the data, there is little point in speculating as to whether the square root transformation for the HV data or T/B_{max} would be the more useful prognostic indicator. It is clear that the information on hypoxia obtained from FMISO-PET makes a contribution to assessment of prognosis. The highest level of FMISO uptake pretherapy, T/B_{max}, reflects the severity of hypoxia and may be most closely related to the biological changes induced by the genomic instability associated with hypoxia. The volume of tissue containing hypoxic cells and the time course of change with treatment may be more related to an oxygen effect on radiosensitivity (29). No one really knows what constitutes “worse” hypoxia, but these alternative variables of hypoxia probably covary within patients.

Most of the patients in this cohort had advanced head and neck squamous cell cancer and, as such, most of them received a combination of radiation therapy and chemotherapy as standard care. Although this contributed to the overall outcome, including variability, it should not have influenced the significant role of pretherapy tumor hypoxia as a predictor of patient outcome. In fact, the wide spectrum of disease and treatment is helpful in generalizing the potential value of FMISO-PET. In view of the established predictive value of metastatic disease (lymph nodal and distant), we looked at the influence of stage at presentation on patient outcome but did not find any significant correlation. Although a larger tumor size at presentation has a negative influence on patient outcome (30), there is evidence that the extent of hypoxia does not correlate with tumor size (19, 29). Our multivariate analysis took into account the tumor and node status as well as T stage in evaluating the influence of FMISO-PET. Although the number of patients and time of follow-up limits our study, it clearly shows a significant role for FMISO-PET as a reliable predictor of survival in patients with head and neck cancer.

Our results indicate different roles for FMISO and FDG, likely due to the nonspecific nature of the FDG uptake mechanism compared with the more specific uptake and retention of FMISO in hypoxic tissues. Although FDG-PET has been proposed as a surrogate marker for hypoxia (31), the heterogeneous cellular response to hypoxia results in significant differences between hypoxia and glycolysis (20, 32, 33). This difference is apparent in Fig. 1.

Advantages of the FMISO-PET study include the availability of F-18, the easy synthesis and availability of an Investigational New Drug for FMISO, a simple method for regional quantification, and its clinical utility. FMISO-PET is becoming a useful tool for clinical applications. The 1.5-hour wait following injection has not limited patient compliance and could be considered analogous to the bone scan in this respect. The quantification by comparison of images to a venous blood sample overcomes any limitations of low image contrast. Other groups have successfully used scoring based on visual image analysis of FMISO uptake (34), but we prefer the normalized image for comparing between patients or comparing images at 2× in the course of treatment. Quantification also provides a continuous variable for monitoring response (35). The specificity of FMISO uptake and retention in hypoxic tissues and the lack of flow dependency are other advantages for its clinical use (12).

Pretherapy information on the oxygenation status of a tumor microenvironment should also have implications for treatment selection. A diffuse distribution of hypoxia in a tumor might suggest benefit from a systemic approach, such as a hypoxic cell cytotoxin, Tirapazamine, or antigrowth factor drugs to combat the limitations of hypoxia (36, 37). Alternatively, a more focal hypoxia might benefit from a local/regional approach, such as intensity modulated radiation therapy–based radiation dose escalation to the hypoxic subvolume (38). We anticipate that FMISO-PET will prove useful for selecting individual patients for the most appropriate treatment.

Acknowledgments

Grant support: NIH grants P01CA42045 and S10 RR17229, and awards from the Medical Research Service and Rehabilitation Research and Development Service, Department of Veterans Affairs, Veterans Health Administration (D. Schwartz).

We thank all nuclear medicine technologists, radiochemists, and physicists in the Division of Nuclear Medicine at the University of Washington Medical Center for their help in PET imaging; Finbar O'Sullivan, Ph.D., Statistician (University College of Cork, Cork, Ireland), for the valuable help in statistical analysis; and Robert Sutherland, Ph.D. (Varian Biosynergy, Mountain View, CA), for the encouragement to study hypoxia.

References

1. Adam M, Gabalski EC, Bloch DA, et al. Tissue oxygen distribution in head and neck cancer patients. Head Neck. 1999; 21:146–53. [PubMed: 10091983]
2. Rasey JS, Koh WJ, Evans ML, et al. Quantifying regional hypoxia in human tumors with positron emission tomography of [18F]fluoromisonidazole: a pre-therapy study of 37 patients. Int J Radiat Oncol Biol Phys. 1996; 36:417–28. [PubMed: 8892467]
3. Brizel DM, Sibley GS, Prosnitz LR, Scher RL, Dewhirst MW. Tumor hypoxia adversely affects the prognosis of carcinoma of the head and neck. Int J Radiat Oncol Biol Phys. 1997; 38:285–9. [PubMed: 9226314]
4. Hockel M, Schlenger K, Knoop C, Vaupel P. Oxygenation of carcinoma of the uterine cervix: evaluation by computerized oxygen tension measurements. Cancer Res. 1991; 51:6098–102. [PubMed: 1933873]
5. Rajendran JG, Wilson DC, Conrad EU, et al. [(18)F]FMISO and [(18)F]FDG PET imaging in soft tissue sarcomas: correlation of hypoxia, metabolism and VEGF expression. Eur J Nucl Med Mol Imaging. 2003; 30:695–704. [PubMed: 12632200]
6. Rudat V, Stadler P, Becker A, et al. Predictive value of the tumor oxygenation by means of pO_2 histography in patients with advanced head and neck cancer. Strahlenther Onkol. 2001; 177:462–8. [PubMed: 11591019]
7. Fyles AW, Milosevic M, Wong R, et al. Oxygenation predicts radiation response and survival in patients with cervix cancer. Radiother Oncol. 1998; 48:149–56. [PubMed: 9783886]
8. Hockel M, Knoop C, Schlenger K, et al. Intratumoral pO_2 predicts survival in advanced cancer of the uterine cervix. Radiother Oncol. 1993; 26:45–50. [PubMed: 8438086]
9. Rofstad EK, Sundfor K, Lyng H, Trope CG. Hypoxia-induced treatment failure in advanced squamous cell carcinoma of the uterine cervix is primarily due to hypoxia-induced radiation resistance rather than hypoxia-induced metastasis. Br J Cancer. 2000; 83:354–9. [PubMed: 10917551]
10. Koh W-J, Griffin TW, Rasey JS, Laramore GE. Positron emission tomography. A new tool for characterization of malignant disease and selection of therapy. Acta Oncol. 1994; 33:323–7. [PubMed: 8018362]
11. Dehdashti F, Grigsby PW, Mintun MA, et al. Assessing tumor hypoxia in cervical cancer by positron emission tomography with (60)Cu-ATSM: relationship to therapeutic response—a preliminary report. Int J Radiat Oncol Biol Phys. 2003; 55:1233–8. [PubMed: 12654432]
12. Rajendran, JG.; Krohn, KA. Imaging Tumor Hypoxia. In: Bailey, DL.; Townsend, DW.; Valk, PE.; Maisey, MN., editors. Positron emission tomography, principles and practice. London: Springer-Verlag; 2002.
13. Dubois L, Landuyt W, Haustermans K, et al. Evaluation of hypoxia in an experimental rat tumour model by [(18)F]fluoromisonidazole PET and immunohistochemistry. Br J Cancer. 2004; 91:1947–54. [PubMed: 15520822]
14. Rasey JS, Koh WJ, Grierson JR, Grunbaum Z, Krohn KA. Radiolabelled fluoromisonidazole as an imaging agent for tumor hypoxia. Int J Radiat Oncol Biol Phys. 1989; 17:985–91. [PubMed: 2808061]
15. Koh WJ, Rasey JS, Evans ML, et al. Imaging of hypoxia in human tumors with [F-18]fluoromisonidazole. Int J Radiat Oncol Biol Phys. 1992; 22:199–212. [PubMed: 1727119]

16. Rasey JS, Nelson NJ, Chin L, Evans ML, Grunbaum Z. Characteristics of the binding of labeled fluoromisonidazole in cells *in vitro*. Radiat Res. 1990; 122:301–8. [PubMed: 2356284]
17. Chapman JD. The detection and measurement of hypoxic cells in solid tumors. Cancer. 1984; 54:2441–9. [PubMed: 6333921]
18. Rajendran JG, Peterson LM, Schwartz DL, et al. [F-18] FMISO PET hypoxia imaging in head and neck cancer: heterogeneity in hypoxia—primary tumor vs lymph nodal metastases. J Nucl Med. 2002; 43:73P.
19. Rajendran JG, Ng P, Peterson LM, et al. F-18 FMISO PET tumor hypoxia imaging: investigating the tumor volume-hypoxia connection. J Nucl Med. 2003; 44:1340–76P. [PubMed: 12902426]
20. Rajendran JG, Mankoff DA, O'Sullivan F, et al. Hypoxia and glucose metabolism in malignant tumors: evaluation by [(18)F]fluoromisonidazole and [(18)F]fluorodeoxyglucose positron emission tomography imaging. Clin Cancer Res. 2004; 10:2245–52. [PubMed: 15073099]
21. Lewellen TK, Kohlmyer SG, Miyaoka RS, Schubert SF, Stearns CW. Investigation of the count rate performance of the General Electric Advance positron emission tomograph. IEEE Trans Nucl Sci. 1995; 42:1051–7.
22. DeGrado TR, Turkington TG, Williams JJ, et al. Performance characteristics of a whole-body PET scanner. J Nucl Med. 1994; 35:1398–406. [PubMed: 8046501]
23. Hamacher K, Coenen HH, Stocklin G. Efficient stereospecific synthesis of no-carrier-added 2-[18F]-fluoro-2-deoxy-D-glucose using aminopolyether supported nucleophilic substitution. J Nucl Med. 1986; 27:235–8. [PubMed: 3712040]
24. Grierson JR, Link JM, Mathis CA, Rasey JS, Krohn KA. Radiosynthesis of fluorine-18 fluoromisonidazole. J Nucl Med. 1989; 30:343–50. [PubMed: 2738663]
25. Kalbfleisch, JD.; Prentice, RL. The statistical analysis of failure time data. New York: Wiley; 1980.
26. Neter, J.; Hunter, MH.; Nachtscheim, CJ.; Wasserman, W. Applied linear statistical models. 4. Chicago: McGraw-Hill/Irwin; 1996. p. 376
27. Kumar P. Tumor hypoxia and anemia: impact on the efficacy of radiation therapy. Semin Hematol. 2000; 37:4–8. [PubMed: 11068949]
28. Thomlinson RH, Gray LH. The histological structure of some human lung cancers and the possible implications for radiotherapy. Br J Cancer. 1955; 9:537–49.
29. Stadler P, Becker A, Feldmann HJ, et al. Influence of the hypoxic subvolume on the survival of patients with head and neck cancer. Int J Radiat Oncol Biol Phys. 1999; 44:749–54. [PubMed: 10386631]
30. Plataniotis GA, Theofanopoulou ME, Kalogera-Fountzila A, et al. Prognostic impact of tumor volume-try in patients with locally advanced head-and-neck carcinoma (non-nasopharyngeal) treated by radio-therapy alone or combined radiochemotherapy in a randomized trial. Int J Radiat Oncol Biol Phys. 2004; 59:1018–26. [PubMed: 15234035]
31. Minn H, Clavo AC, Wahl RL. Influence of hypoxia on tracer accumulation in squamous-cell carcinoma: *in vitro* evaluation for PET imaging. Nucl Med Biol. 1996; 23:941–6. [PubMed: 9004282]
32. Rajendran JG, Krohn KA. Imaging hypoxia and angiogenesis in tumors. Radiol Clin North Am. 2005; 43:169–87. [PubMed: 15693655]
33. Dehdashti F, Mintun MA, Lewis JS, et al. *In vivo* assessment of tumor hypoxia in lung cancer with 60Cu-ATSM. Eur J Nucl Med Mol Imaging. 2003; 30:844–50. [PubMed: 12692685]
34. Rischin D, Peters L, Hicks R, et al. Phase I trial of concurrent tirapazamine, cisplatin, and radiotherapy in patients with advanced head and neck cancer. J Clin Oncol. 2001; 19:535–42. [PubMed: 11208848]
35. Rajendran JG, Muzi M, Peterson LM, et al. Analyzing the results of [F-18] FMISOPET hypoxia imaging: what is the best way to quantify hypoxia? J Nucl Med. 2002; 43:102P.
36. Brown JM. Exploiting the hypoxic cancer cell: mechanisms and therapeutic strategies. Mol Med Today. 2000; 6:157–62. [PubMed: 10740254]
37. Peters LJ. Targeting hypoxia in head and neck cancer. Acta Oncol. 2001; 40:937–40. [PubMed: 11845958]

38. Rajendran JG, Meyer J, Schwartz DL, et al. Imaging with F-18 FMISO-PET permits hypoxia directed radio-therapy dose escalation for head and neck cancer. J Nucl Med. 2003; 44:415, 127.

Fig. 1.

FMISO and FDG-PET images (coronal) of a 70-year-old patient with a primary piriform sinus squamous cell carcinoma (*solid arrow*) with metastatic lymph nodes (*open arrows*).T/B_{max} is 1.5. HV is 6.44 mL for the primary tumor.

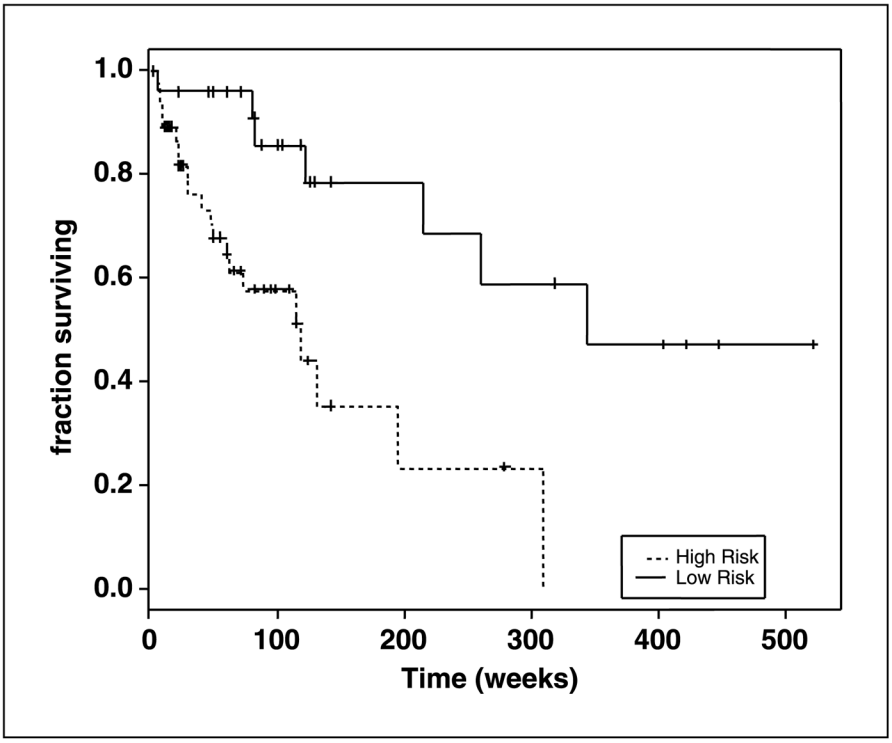

Fig. 2.

Kaplan-Meier overall survival curve when patients are classified by the presence of nodes. High risk (n = 46) is defined as having N_2 or N_3 disease.

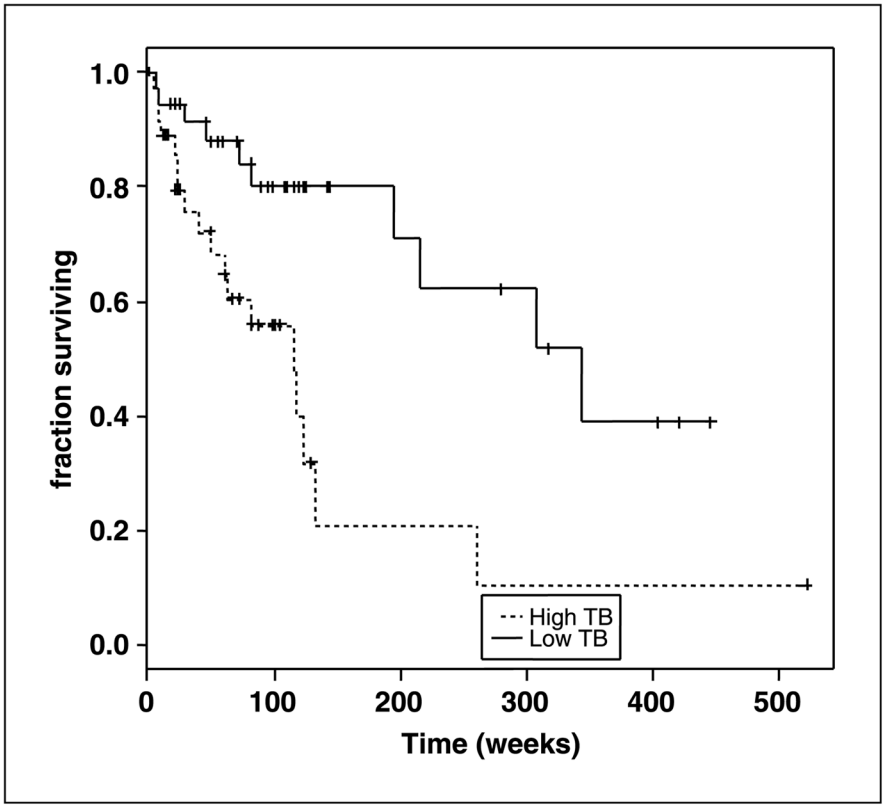

Fig. 3.

Kaplan-Meier overall survival curve when patients are classified byT/B_{max}. High T/B_{max} is defined as patients whose T/B_{max} is above the median of 1.5.

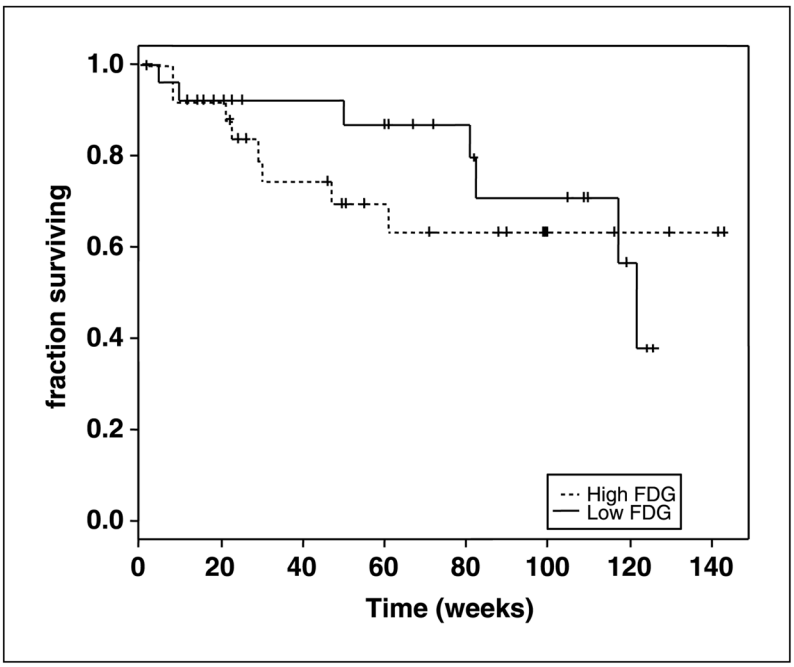

Fig. 4.

Kaplan-Meier overall survival curve when patients are classified by FDG uptake. High FDG is defined as patients whose FDG uptake is above the median SUV_{max} of 10.4.

Table 1

Tumor-node-metastasis staging categorization for patients with head and neck cancer (n = 73)

	N_0	N_1	N_2	N_3	Total
T_x	0	0	3	0	3
T_1	4	0	2	2	8
T_2	3	3	10	3	19
T_3	4	5	9	1	19
T_4	5	3	13	3	24
Total	16	11	37	9	73

Table 2

Summary of univariate statistics for Cox regression model

Univariate statistics for Cox regression: overall survival							
Variable	**Mean (SD)**	**Hazard ratio**	**Lower 0.95 confidence limit**	**Upper 0.95 confidence limit**	***n***	**Events**	***P***
Node stage	—	1.84	1.17	2.87	73	28	**0.01**
Tumor stage	—	1.33	0.89	1.98	70	26	0.17
Age	61.1 (10.4)	1.10	0.81	1.50	73	28	0.55
FDG SUV_{max}	10.8 (4.5)	1.44	0.88	2.37	52	15	0.14
T/B_{max}	1.6 (0.46)	1.68	1.22	2.32	73	28	**0.002**
sHV*	2.8 (2.4)	1.46	1.01	2.11	69	25	**0.04**

NOTE: For the continuous variables, the hazard ratio and the confidence intervals should be interpreted as the increase in survival risk associated with an increase of 1 SD of the independent variables. *P* values for significant variables are in bold type.

*For statistical purposes only, a square root transformation was used on the HV data (sHV).

Table 3

Summary of multivariate statistics for full Cox regression model for patients who had both FMISO and FDG scans

Multivariate Cox regression analysis results: overall survival, *n* = 50, deaths = 14				
Variable	**Hazard ratio**	**Lower 0.95 confidence limit**	**Upper 0.95 confidence limit**	***P***
Node stage	2.09	0.98	4.44	0.06
FDG	1.64	0.95	2.83	0.08
Tumor stage	1.26	0.66	2.42	0.48
Age	1.52	0.80	2.91	0.20
T/B	1.97	0.99	3.93	0.06

NOTE: Median follow-up for this data set was 61 weeks. For the continuous variables, the hazard ratio and the confidence intervals should be interpreted as the increase in survival risk associated with an increase of 1 SD of the covariate (refer to Table 2 for SD values).

Table 4

Summary of reduced Cox regression model for all patients who had FMISO scans

Multivariate Cox regression analysis results: overall survival, *n* = 73, deaths = 28				
Variable	**Hazard ratio**	**Lower 0.95**	**Upper 0.95**	***P***
Node	1.77	1.10	2.85	**0.02**
T/B	1.57	1.14	2.17	**0.01**

NOTE: Median follow-up for this data set was 72 weeks. For the continuous variables, the hazard ratio and the confidence intervals should be interpreted as the increase in survival risk associated with an increase of 1 SD of the covariate (refer to Table 2 for SD values). Significant variables are in bold type.